Rubidium isotope shift measurement made simple

A. Anderson,* T. Ayers,† B. E. Bish,‡ S. Cart,§ V. Tobar Correa,¶ A. O'Brien,** R. Stipanovich,†† and M. Crescimanno‡‡

Department of Physics and Astronomy,

Youngstown State University, Youngstown, OH, 44555

(Dated: November 24, 2025)

Abstract

Experimentally determining the isotope shift leads students beyond their naive understanding of atomic structure and can introduce them to the basics of optical metrology. Earlier undergraduate laboratory experiments for the isotope shift on the principal D1 and D2 transitions in Rubidium typically relied on saturated absorption spectroscopy. We show that using a different atomic state, namely the $5D^{5/2}$ level significantly simplifies the data collection, analysis and interpretation all the while yielding a measurement within two percent of the accepted value. Using nothing more than free-running laser diodes, a cell, a few low-bandwidth photodiodes and a Fabry-Perot cavity this laboratory experience impells students to recognize the necessity of a third (beyond the effect of the nucleus's countermotion and the finite nuclear charge radius) many-body quantum mechanical contribution to the isotope shift, the specific mass shift.

I. INTRODUCTION:

The utility of including an isotope shift measurement in the undergraduate laboratory is that it refines and expands the atomic physics lessons that the students learn as part of their junior/senior (quantum-) physics sequence. Asking undergraduate physics majors about their 'picture' of the atom often reveals common misconceptions, among them the notion that the nucleus 'sits' at the center of a symmetrical electron cloud. If so, then why would the mass of the nucleus itself play any role in the electronic excitation spectrum? Of course, an appeal to their classical understanding reveals that the nucleus/atomic core must indeed be in countermotion to the electron, which in the S-state is continually moving radially; a laboratory experience measuring the isotope shift reinforces this 'picture' of co-motion inside the atom, but also goes beyond it. Isotope shift measurements in the optical section of the undergraduate advanced laboratory appears to have traditionally been done by comparing the hydrogen and deuterium Balmer series using a monochromator and a photomultiplier tube (PMT)[1] although relatively low cost, compact, medium resolution spectrometer also suffice. Doing so one recovers the aforementioned effect of the nuclear orbital co-motion without being sensitive to the much smaller isotope nuclear size effects. In contrast, experiments using rubidium's brightest transitions at 780nm (D2) and 795nm (D1) contain both the effect of the core's countermotion and the nuclear size effects as well as a third contribution called the specific mass shift (SMS) that is a more subtle consequence of the multi-electron wavefunction for that state. We note that in older literature the SMS term is sometimes called the "mass polarization" term.

We present a greatly simplified approach to the isotope shift measurement by using a free-running 776nm laser in conjunction with a 780nm laser to excite and study the shift in a 2-photon excited state, the $5D^{\frac{5}{2}}$ state. The spectral compactness of the hyperfine states of the $5D^{\frac{5}{2}}$ makes the data analysis more straightforward for the students and allows one to experimentally unambigiously distinguish the SMS contribution. The approach we describe here is simple in that it uses only standard laboratory-grade photodiode detectors (no PMT) and COTS optics.

Laser diodes have long been used in hyperfine spectroscopy on both of the principal near infrared optical transitions (called the "D1" at 795nm or "D2" at 780nm respectively (Fig.3, purple (middle) trace). The use of SAS technique on these transitions in measuring

the isotope shift forms extensive existing literature typically employing Extended Cavity Diode Lasers (ECDLs)[2,3], or somewhat more intricate cavity stabilized schemes.[4,5] For more details on the physics of the laser diode and the historical development of their use in atomic spectroscopy see Ref.[6]. There is significant literature on SAS's use in higher excited state levels, notably[2,7–10], and even pulsed lasers, for example in Ref.[4,11], as well as for other atomic species[12], even with free-running (non ECDL) laser diodes.[13,14] Quantifying the isotope effect on the 780nm (D2)/795nm (D1) fine structure split transitions in Rubidium also has a celebrated history[15–21] (read Ref.[22] for a more up-to-date experimental summary of isotope shift measurements specific to rubidium), and more recently precision measurements of the isotope shift have been of interest for the indirect detection of new physical interactions.[23–25]

Measuring the isotope shift using higher excited states via two-photon transitions in Rubidium hails from the mid 1970's.[16,26] These early measurements were meant primarily as surveys and had uncertainties that were large by modern standards (large also in comparison with the method described here). A much more accurate measurement of the isotope shift through the use of a rather elaborate microwave standard referenced frequency chain was first possible in the 1990's, which reported the isotope shift for the state of interest for the current paper, the $5D_{\frac{5}{2}}$ state in Rubidium, of 163.033 (6) MHz.[27] That team was able to use their setup to measure a whole host of shifts in different levels and different atomic species, with about the same accuracy. The advent and diffusion of frequency combs has significantly extended the precision of other efforts to measure isotope shifts, including in the 6P levels of Rubidium.[28] Turnkey frequency combs systems are still rather expensive and their use in this application requires heterodyne detection and signal recovery technique beyond that typically taught in an undergraduate advanced laboratory.

Over the last 20+ years basic laser diode spectroscopy technique has become part of the cannon of the advanced undergraduate laboratory.[29] Of particular interest beyond measuring the isotope shift, laser diode spectroscopy has been used to teach about Doppler broadening[30] , radiative broadening[31], non-linear spectroscopy[32], noise spectroscopy[33] and SAS lineshape.[34,35]

This experiment uses commodity Indium Gallium Arsenide near infrared laser diodes for which the emission wavelength (∼780nm) varies smoothly with temperature and current over limited ranges, punctuated by large abrupt changes called "mode hops". Mode hops arise from the temperature-induced relative change of the laser diode's Fabry-Perot

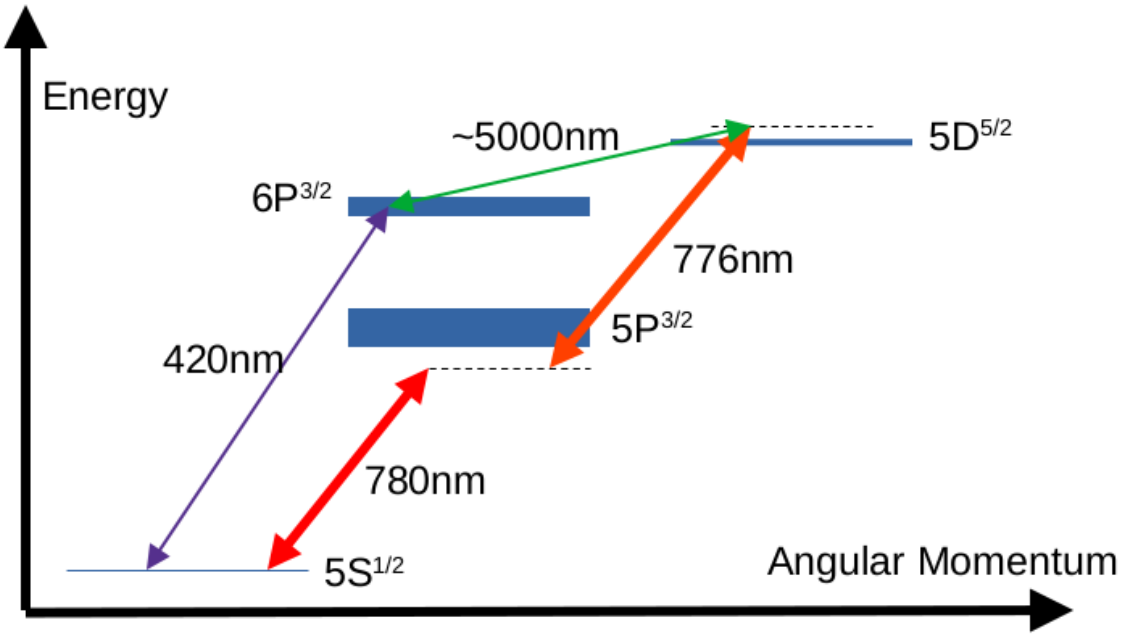

FIG. 1. The level structure of atomic Rubidium with laser transitions of relevance this report. Hyperfine atomic sublevels are not shown individually, but their energy spread is indicated by the level widths (not to scale). The doppler effect allows the two-photon process used here to connect the S and D state even with significant one-photon detuning. For the doppler (nearly-) free configuration used in this report only the sum of the frequencies of the 776nm and 780nm laser need be within the D state's hyperfine manifold.

resonances relative to the intrinsic gain envelope of the semiconductor. These hops not withstanding, we have found that about a fourth of the 780nm diodes we have cooled with a thermoelectric coolers (TEC) are tunable onto 776nm 5P-5D transition in Rubidium. For our use here, an admittedly crude temperature stabilization suffices, allowing those interested in implementing this laboratory to avoid the additional cost and optical/mechanical complexity associated with making these 776nm sources into ECDLs.

Comparing a pair (or more) of transitions on a pair of isotopes one can determine the three distinct contributions to the isotopic difference: (1) the NMS, or normal ("naive") mass shift (from the nuclear countermotion of the excited atomic core about the center of mass of the unexcited atom), (2) the NS , or nuclear "field shift" (due to the spatial structure of the charge density in the nucleus) and (3) the so-called specific mass shift (SMS). The first two contributions are rather easy to conceptualize and determine using

the D1 (795nm) and D2 (780nm) in SAS[14]. However with those measurements one cannot easily disentangle the SMS contribution as a distinct contribution. The SMS contribution is somewhat harder for students to conceptualize. It is a consequence of changes in the many-body electronic kinetic energy in going from one isotope to another, and so is intrinsically a (many body-)wavefunction effect. For some recent examples of experimental accounting for these contributions see Ref.[36] for Neon and Ref.[37] for excited states of atomic Titanium. One advantage of measuring the isotope shift via a second excited state, such as the $5D^{5/2}$ as presented here, is that it leads students rather directly to an estimate of the SMS as a distinct contribution.

We have already mentioned that, at the complexity "cost" of making and tuning the 776nm laser, the resulting interpretation and computation of the associated isotope shift is simpler than for the 5P levels. Note also that the earlier 5P level SAS version of this lab one had a systematic error from the visibility of unresolved 5P hyperfine states. These contributions are often ignored in computing the "center of mass" of the excited state manifolds due to their generally poor visibility. In Ref.[14] it was noted that if one includes as a naive frequency estimate for these "missing" transitions ^{85}Rb F=3 $\rightarrow$ F'=1 and the ^{87}Rb F=2 $\rightarrow$ F'=0 as being as far in energy from their neighbor (the ^{85}Rb F=3 $\rightarrow$ F'=2 and the ^{87}Rb F=2 $\rightarrow$ F'=1) as those states are in turn from their respective neighbors (the ^{85}Rb F=3 $\rightarrow$ F'=3 and the ^{87}Rb F=2 $\rightarrow$ F'=2), one finds an isotope shift of 79 MHz (resulting in a ground state energy shift of 172 MHz), somewhat nearer to the accepted value.

The experiment we describe uses a free running commodity laser diode which has a linewidth that is roughly the same as the 5D excited state hyperfine intervals. In practice this leads to a determination of the isotope shift that is within a MHz or so of the value known from precision experiment, and is thus inherently more accurate than the common approach based on Saturated Absorption Spectroscopy.[14] In the approach detailed below, since a higher excited state is used, the hyperfine splittings of that state are small so that one may approximate the entire optical response as if it were a single state; it is as if the convolution of the intrinsic atomic lineshape with the free-running 776nm laser's frequency spread already comprises the excited state weighted sum (as in Eq.6 for the ground state) needed in computing the isotope shift. Then it suffices to identify only a single composite transition of the 5D level for each isotope's two ground state hyperfine levels. Although the free running laser linewidth of several MHz sounds like a disadvantage it greatly simplifies

the student's interpretation and computation. By going to the next level of analysis and quantifying the lineshape distortion associated with these overlapping excited state hyperfine components, we show why ignoring this excited hyperfine sub-structure works as well as it does.

II. THEORY:

In its simplest form, the isotope shifts in an elemental spectrum are the result of the nuclear countermotion, the nuclear charge distribution and changes in the many-body electronic contribution to the kinetic energy. Students will be familiar with the fact that the energy levels of the hydrogen atom are proportional to the reduced mass $\mu = mM/(m+M)$ where m is the electron mass and M is the nuclear mass. Rubidium, being hydrogen-like (in having a mostly isolated single electron in its outmost shell) then, to leading order, is expected to also have energies proportional to μ. This μ-scaling of the first term in the energy in literature is referred to as "the normal mass shift" , or NMS. Of course, that formula assumes that all the charge is at $r = 0$, whereas the nuclear charge is effectively spread out over roughly a fermi. This causes a deviation from a pure Coulomb potential that also perturbs the state energies, primarily of the S-wave electronic states which have "penetration at the nucleus" and so can – in perturbation theory – 'see' this deviation from a pointlike nuclear charge. This non-nuclear mass related effect is called the "nuclear shift" or NS contributions. This effect is sometimes referred to in the literature as the "field effect" term.

The third distinct contribution, called the "Specific Mass Shift" or SMS is from secondary differences in the multielectron wavefunction between isotopes. These arise from the multielectron kinetic term changing slightly between isotopes. Unlike the other two contributions (NMS and NS), the SMS is harder to conceptualize, being a consequence of the effect that the wavefunction change from the NS, filtered through the Fermi symmetry of the full many-body wavefunction, has on the kinetic terms.[38]

To illustrate the SMS contribution to the isotope effect consider a one-dimensional 3 body quantum mechanics problem involving one nucleus and a pair of identical fermions. We regard the fermions as 'spinless' in that we require full antisymmetrization under exchange

but do not include any internal contribution to the wavefunction. The Hamiltonian reads

$$H = \frac{P^2}{2M} + \frac{p_1^2}{2m} + \frac{p_2^2}{2m} + V(R - r_1) + V(R - r_2) + V_f(r_1 - r_2) \tag{1}$$

where P (p_i , $i = 1, 2$) is the momentum of the nucleus of mass M (fermions mass m, respectively). In separating the center of mass motion out from the relative motions, one finds a re-organization of the quadratic terms:

$$H = H_{cm} + \frac{\pi_1^2 + \pi_2^2}{2\mu} + \frac{\pi_1 \pi_2}{M} + V(x_1) + V(x_2) + V_f(x_1 - x_2) \tag{2}$$

where π_i is the momentum conjugate to the relative co-ordinates $x_i = r_i - R$, and μ is the single particle reduced mass $mM/(M + m)$. The $\frac{\pi_1 \pi_2}{M}$ is the SMS term that leads to a shift beyond the nuclear and normal isotope shifts discussed earlier.

For an analytically solvable example of the SMS contribution, consider the harmonic case $V(x) = \frac{1}{2}Kx^2$ and $V_f = 0$. The multiparticle wavefunction for the ground state is now of the form $\psi_0(x_1, x_2) = A_0(x_1 - x_2)e^{-\alpha(x_1^2 + x_2^2) + \beta x_1 x_2}$, and that for the first excited state is $\psi_1(x_1, x_2) = A_1(x_1^2 - x_2^2)e^{-\alpha(x_1^2 + x_2^2) + \beta x_1 x_2}$, where $\alpha > 0$ and β are assumed to be real and A_i are normalization constants. The requirement $H\psi = E\psi$ indicates

$$\frac{4\alpha^2 + \beta^2}{\mu} - \frac{4\alpha\beta}{M} = K \qquad\qquad 4M\alpha\beta = \mu(4\alpha^2 + \beta^2) \tag{3}$$

And so the computed energy difference

$$E_1 - E_0 = \sqrt{\frac{K(M + \mu)}{\mu M}} \tag{4}$$

This model clearly does not contain a nuclear shift (NS). Regarding the above energy difference as a sum of a NMS (expected as $\sqrt{\frac{K}{\mu}}$) and a SMS contribution only, we learn their ratio is

$$\frac{\text{SMS}}{\text{NMS}} = \sqrt{1 + \frac{\mu}{M}} - 1 \tag{5}$$

from which we see that at small $\frac{\mu}{M}$ the SMS is negligible, is always positive, monotonic and is smaller than the NMS at all values of the mass ratio but can grow to a substantial fraction of the overall shift at large mass ratios.

Although the forgoing example using harmonic potentials has the advantage of allowing an exact evaluation of the isotope shift and SMS contribution, consider now the (more closely related to experiment) computation of the isotope shift between H^- and D^- in perturbation

theory, ignoring the NS (nuclear size effect) term. The Hamiltonian is that of Eq.2 with $V(x) = ke^2/x$ and we again neglect $V_f = 0$. Working perturbatively in μ/M, we can take as a one-particle basis set the hydrogen (single electron) wavefunctions from which to build the multi-electron states. For example, consider the ground state singlet $1s^2$. Treating the $\frac{\vec{\pi}_1 \cdot \vec{\pi}_2}{M}$ in perturbation theory we have for the leading contribution to the state's energy $E^{(0)} = -\alpha^2 \mu c^2$ and a first order energy shift $E^{(1)} = -\frac{\hbar^2}{M a_\mu^2}$ where $a_\mu = \frac{\hbar^2}{\mu e^2}$ and α is the fine structure constant. Combining we have, $E = E^{(0)} + E^{(1)} + \ldots = -\alpha^2 c^2 (\mu + \frac{\mu^2}{M}) + \ldots$ which expanding in $m/M << 1$ is just $E = -\alpha^2 c^2 m$ and so the $1s^2$ exhibits no leading order isotope shift.

It is tempting to understand this lack of an isotope shift intuitively via the classical picture that these S electrons are on strictly radial orbits and the overall minus sign of the $\frac{\vec{\pi}_1 \cdot \vec{\pi}_2}{M}$ term when evaluated on this state to this order indicates that the two electrons are on average in synchronized oppositely directed radial motions. Were that the case there would be no net nuclear countermotion, explaining the resulting independence of the energy on the nuclear mass. This interpretation of the above calculation is too naive, as computing the SMS term on the singlet $2s^2$ state (see[20] however reprised in[39,40] and more recently in[41]) for which we find $E = -\frac{\alpha^2 c^2}{4}(\mu + 2\frac{\mu^2}{4M})$ in this approximation. Furthermore when the electronic states are different this argument provides no insight as to the magnitude of the effect, for another example the perturbative calculation of the energy of the (singlet or triplet) $1s^1\ 2p^1$ has $E = -\frac{\alpha^2 c^2}{8}(5\mu + 2\frac{\mu^2}{M})$ which also has M dependence to leading order coming from both the NMS and SMS.

In any case, for real atoms a host of other significant effects (for example, the changes in the wave function associated with the electron-electron interaction, leading order relativistic effects, hyperfine interaction, etc.) that lead to isotope shifts of the state energies. With regard to the electron spin and magnetic moment of the isotope's nucleus (hyperfine interaction effects) the states are organized only by the total angular momentum quantum number $F = I + j + S$. Although one cannot ignore these effects for the Rubidium atom, one can "average out" these magnetic splittings completely by forming state-weighted linear combination of the energies, $\mathrm{n}E_{0HFS\ ^{d85}Rb} = (7f_{85Rb\ F=3} + 5f_{85Rb\ F=2})/12$ for ^{85}Rb and $E_{0HFS\ ^{87}Rb} = (5f_{87Rb\ F=2} + 3f_{87Rb\ F=1})/8$ for ^{87}Rb as dictated by the I of 5/2 and 3/2 respective nuclei. These so-called 'center of mass' energies then represent the energy of the atomic state were the electron spinless (i.e non-magnetic). These 'synthetic' hyperfine

interaction-independent energy levels that result from this multiplicity-weighted averaging are then compared between isotopes for the experimental reporting of the transition isotope shift.

III. EXPERIMENT:

Although the resulting simplicity of the dataset and its interpretation make this laboratory an attractive addition to or substitute for an isotope shift measurement laboratory, perhaps the biggest hurdle to its widespread implementation is the creation and tuning of the 776nm diode laser source. It is actually not too difficult to build a 776nm diode candidate laser starting from almost any diode that at room temperature is close to 780nm. We use the qualifier "candidate" because in our experience not every diode can function reliably at that wavelength and even if it does, it may 'mode hop' over the wavelengths of spectroscopic interest. We have found in practice that one out of about every four diodes can be brought into resonance with the 776nm $5P^{3/2} \rightarrow 5D^{5/2}$ transition in Rubidium.

The diode was mounted in a drilled hole in a thin (2mm thick) aluminum 'T'. On one of the flanges a small outcoupling mirror was mounted (at 45 degrees to the flange). On the stem of the "T" next to the diode a small divot was drilled into the aluminum into which an 10KΩ excapsulated NTC thermistor (a NCP15XH103F03RC negative temperature coefficient thermistor) was afixed. The 'T' is then inverted, and first loosely held in place with a thin thermal paste to a 2mm thick aluminum plate that matched the dimensions of the face of a $<$ 8amp thermoelectric Peltier-effect cooler (TEC). The whole plate is then affixed to the TEC with thermal paste, and the other side of the TEC is also pasted and mated with an expanded aluminum heatsink. A mounting hole for holding the assembly is made in the heat sink and the multilayer "sandwich" with the diode and thermistor and mirror in the inverted "T", TEC and heatsink is fastened together with thermally non-conducting restraint band (nylon zipties suffice) and then housed in a styrofoam cover, mostly to limit infiltration of warm air. A thin pellicle of glass can be mounted above the outcoupling mirror to further limit infiltration or air, though often that is not necessary.

A low resolution spectrometer is used to help determine a crude temperature set point for the control loop to keep the laser near 776nm. For simplicity we chose to write a PID program (available at[43]) for an Arduino Uno for temperature control. It uses an analog input

pin on the Arduino to read the divided voltage from a single 10KΩ resistor in series with the laser package's thermistor. This pair is driven by the rather poorly regulated 5V output from the Arduino. The voltage reading is used to to set the pulse-width modulated (PWM) duty cycle pulses the Arduino sends to the gate of a single mosfet in series with the TEC and a DC supply (12V). Clearly there are many options to improve on this sufficient but bare-bones laser diode temperature control, but parsimony of parts and ease of modification are its strength.

Once the Arduino-based laser temperature controller is tuned via code, a few minute warm up is all that is needed to get the lab ready for the students. Then, from the student point of view, this lab looks rather straightforward in that the most challenging alignment task is overlapping the counterpropagating beams in the vapor cell (A natural abundance vacuum cell, 10cm length and 2.5cm diameter, unshielded and held at a fixed temperature between 45-80^{o}C) and the adjustment/alignment of the Fabry-Perot (FP) cavity. In the most basic implementation of this laboratory all the data can be readily taken with two slow-speed (0.3mm-square, amplified 5MHz bandwidth) photodetectors hooked to a 2-channel scope (though we found it convenient to use a 4-channel Siglent SDS1204X-E).

First, during a slow (10-100 Hz) current sweep of the 780nm laser, one photodetector receives the 780nm absorption signal from the SAS cell setting the sweep parameters based on the known frequency interval between the SAS resonances in 85Rb. The second photodetector reads the transmission of the FP cavity. We used a relatively low finesse ($\sim$150) confocal 20cm aluminum-body FP cavity not in a temperature regulated enclosure (FP made by Teachspin). Based on these data the free spectral range (FSR) of the FP cavity was measured to be 394$\pm$2 MHz in our experiment. In our implementation the 780nm beam had a total power of 1.4 mW and a diameter at the cell of 1.5mm at the cell window while the 776nm beam had a total power of 0.4mW and a much smaller diameter, $<$ 0.5mm in the cell. We note that the spatial structure of the 780nm beam was much better than the 776nm laser and a 0.75m focal length convex lens upstream from the cell was used to collimate the 776nm down to the reported size in the cell.

The photodetector that was collecting the SAS signal is then moved to measure the transmission of the 776nm beam during the 780nm sweep. Both lasers are driven with commercial stable current supplies. The 776nm laser current was driven by a Thorlabs LDC500 and is not swept. The drift rate of the 776nm laser in the thermal enclosure regulated by

the Arduino code with this current drive was less than 5MHz/s, as we directly verify in the dataset below. We found it useful to AC couple the scope input to the photodetector measuring the transmission of the 776nm. The 780nm laser was swept (by a ∼1mA triangle wave ontop of a 55mA DC current), and visually checking the regularity of its FP data indicates that the laser's frequency scan is likely to be free of frequency mode hops. Although the 780nm laser we used was a commercial ECDL, we had no need to modulate the grating peizo, as current modulation was sufficient to span the 10 GHz frequency range without modehops. Being particularly sensitive to back-reflection, we found that a linear polarizer followed by a quarterwave plate upstream was a sufficient reflection isolator to stabilize the 780nm laser from the rest of the experiment during the sweeps. A different waveplate in a rotary mount was placed upstream of the experiment on the 776nm beam, not for isolation, but to adjust and optimize the signal (absorption changes). Little attention was paid to the polarization dependence of the signal since the changes from polarization choices did not seem so pronounced. All the signal traces are taken quite slowly, and no cable termination was necessary. The DC and triangle AC components of the 780nm diode current were ad-

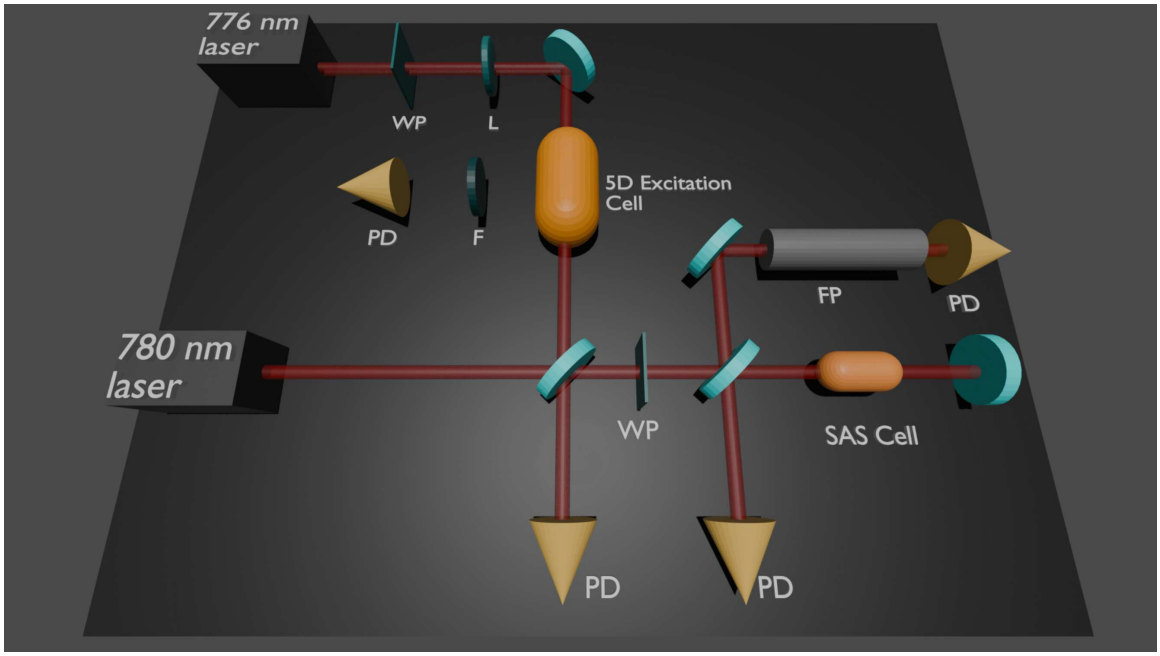

FIG. 2. Experimental Setup: Rb rubidium vapor cell, FP Fabry-Perot cavity, PD photodiodes, BS non-polarizing beam splitter, WP waveplate, F 420nm notch filter (optional), L lens

justed until the laser's output scanned a mod-hop free frequency range that spanned the

ground state hyperfine states of ^{87}Rb. The 780nm pump and 776nm probe beam counter-propagate and overlap inside the vapor cell. Then during the 780nm sweep four distinct 776nm absorption peaks appear, one for each ground state hyperfine level (F=2,3 for 85Rb surrounded by F=1,2 of 87Rb) as in Fig. 3. The reason there are only 4 is that the hyperfine splitting in the $5D^{5/2}$ manifold (10's of MHz) is much smaller than the hyperfine splitting in the $5P^{3/2}$ manifold (typically 100MHz) combined with the fact that the free-running 776nm laser's bandwidth is probably in the multi-MHz range. This indicates that the 776nm laser's propagation through the vapor when in resonance cannot resolve the individual hyperfine components of the $5D^{5/2}$ state whereas, in this counter-propagating configuration, it is spectrally pure enough to only connect a single motional $5P^{3/2}$ hyperfine state with the $5D^{5/2}$ states. Furthermore, since the two lasers are so close in frequency, the Doppler offset on the two-photon resonance can be neglected, being essentially the same for each resonance. Such an offset shifts the overall four distinct peaks but cancels out of the isotope shift measurement, significantly simplifying the analysis.

On the other hand, a linear drift in the 776nm laser's frequency during the trace would lead to a systematic error in the isotope shift. In practice this can greatly reduced by care in tuning the control loop for the temperature of the diode and increasing the sweep rate. A constant drift rate can be removed entirely by averaging the isotope shift computed during the up-chirp (Fig.3, $t \in [.006 - .014]$) with that of the down-chirp (Fig.3, $t \in [.014 - .022]$).

The traces are stored digitally and subsequently analyzed by filling out a table of the temporal locations of each FP transmission resonance and the center of each 776nm absorption feature (which were fit by Gaussians). Best practice for assigning an (offset) frequency to each absorption feature, as described throughout the literature, is not to fit the FP data for a single function of frequency versus sweep time, but instead to simply count whole FSR's (FP resonances) up to the absorption feature and then interpolate across the nearest neighbor FP resonances to the feature's center.

With these measured offset frequencies one can then assemble the isotope shift for this state by taking the difference between the "centers of mass" of the spectra of each isotope, as described in the earlier theory section,

$$\text{Isotope Shift} = (5f_{87Rb\ F=2} + 3f_{87Rb\ F=1})/8 - (7f_{85Rb\ F=3} + 5f_{85Rb\ F=2})/12 \qquad (6)$$

yielding for a set of 10 runs shown in Fig.4 an isotope shift for this state of about 163±1

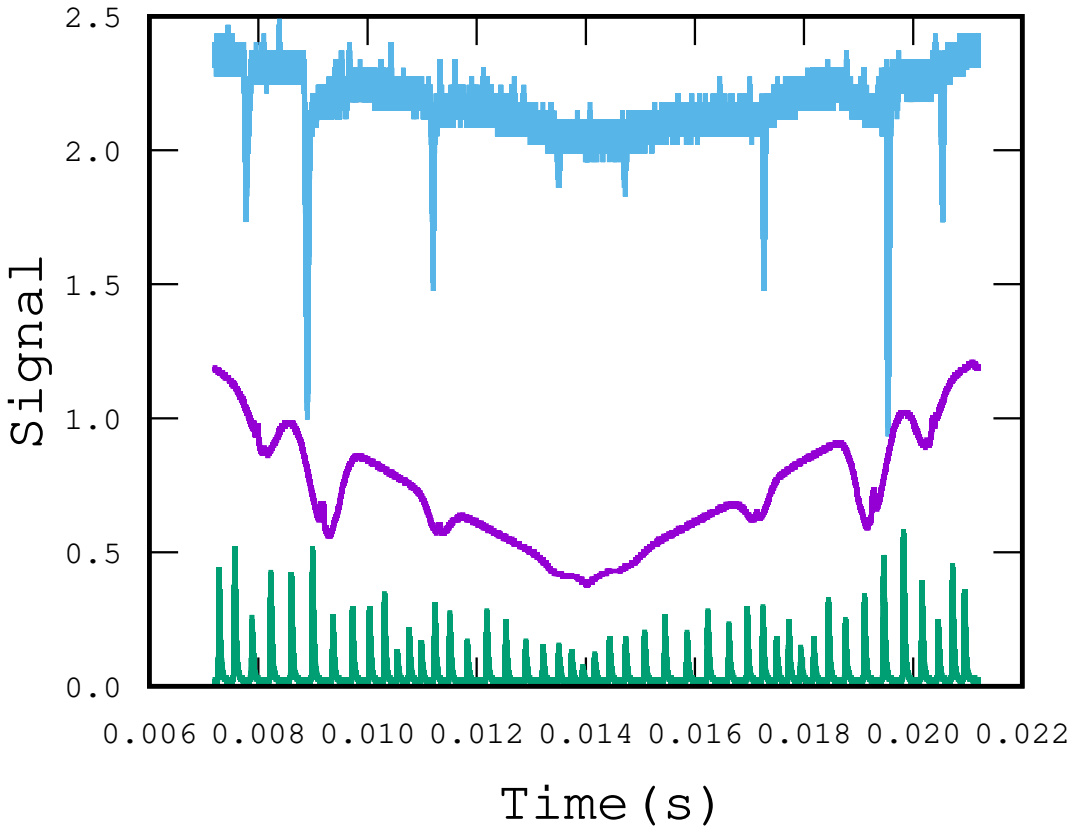

FIG. 3. Typical Oscilloscope traces while 776nm laser (its transmission in blue, top) is held fixed and the 780nm laser is swept (its transmission in purple, middle). The green trace (bottom) is the output of the Fabry-Perot cavity illuminated by a portion of the 780nm laser field. Datasets vertically offset for clarity.

MHz.

Many versions of this experiment use a 420nm filter coupled with a photomultiplier tube (PMT) to directly measure the flourescence from the $6S^{3/2}$ state in the decay chain of the $5D^{5/2}$. We note that the experiment we report on here made no use of a PMT, but instead a slow amplified photodector behind a 420nm notch filter sufficed to record the flourescence, even at these low powers (see Fig.5). The human eye also works well in this regard, as students enjoy seeing the blue trace through the notch filter, even recording it on their cell phones during a sweep.[42]

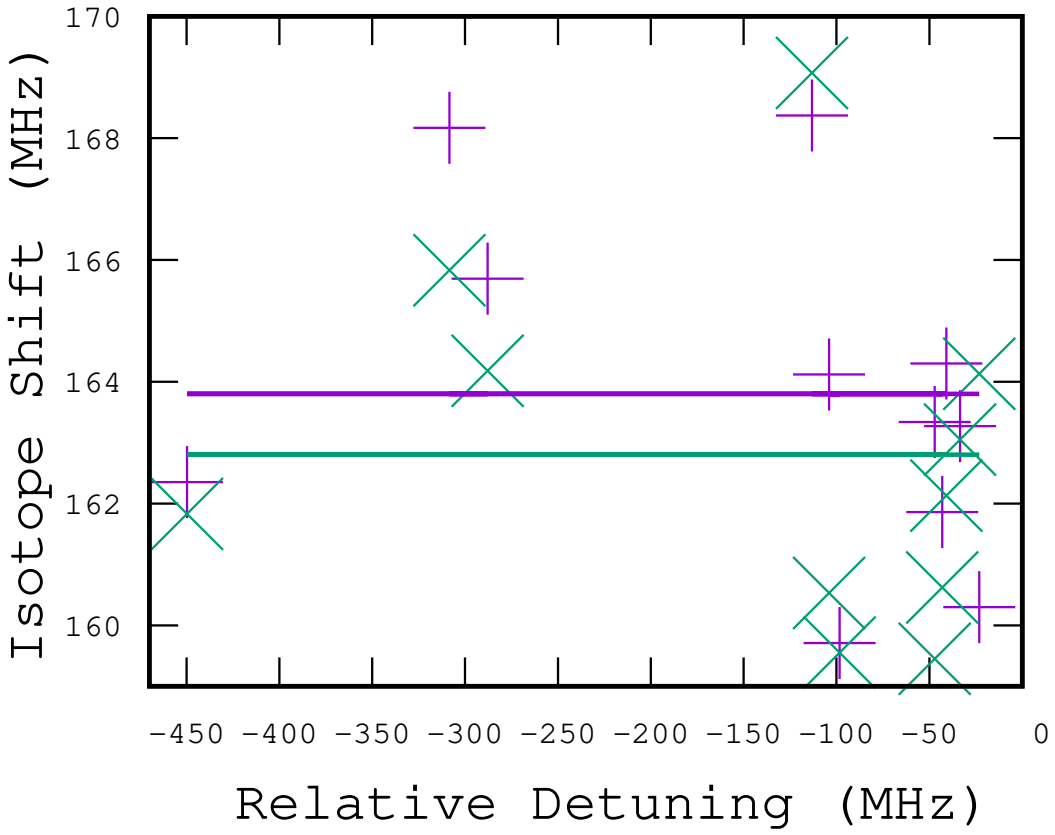

FIG. 4. Eleven different measurements of the isotope shift of the $5S^{1/2}$ to $5D^{5/2}$ interval between ^{87}Rb and ^{85}Rb as a function of the 776nm detuning. The green 'x' are using the centers from the full gaussian fit of the FP resonances, whereas the "+" are the result of using just the FP resonance maxima. The colored lines are the averages for of each dataset and represent 163.8±0.8 and 162.8±0.9 MHz respectively

IV. ANALYSIS AND STUDENT EXPERIENCE

A complete example of the isotope shift calculation can be summarized for the data depicted in Fig.3. Call the FP resonance (purple) before the first ^{87}Rb (the F=2) at time -0.048s zero frequency. Then the 776nm absorption (blue line in figure) feature from the nearby ^{87}Rb line is nearly 1/4 of a FP FSR. The associated ^{87}Rb 776nm absorption feature (in blue, near -0.008s) is at 16.8 FSRs later. Thus, the $(5f_{87Rb\ F=2} + 3f_{87Rb\ F=1})/8 =$ 6.46 FP FSRs. For the ^{85}Rb lines at approximately 3.5 and 11.6 FSR gives $(7f_{85Rb\ F=3} + 5f_{85Rb\ F=2})/12 = 6.87$ FSR, so that the isotope shift is -0.419 FSR, or equivalently, about -165MHz.

To understand the sign recall that we are sweeping the 780nm laser, and holding the 776nm laser at fixed frequency during the ramp. Since they are counterpropagating and thus here nearly Doppler free (being of nearly the same frequency), a negative shift as seen in the 776nm relative to the sweep indicates a positive frequency displacement of the 780nm. The sign indicates that the overall energy difference between the $5S^{1/2}$ and the $5D^{5/2}$ is such that in the above example, the measured interval $5S^{1/2}$-$5D^{5/2}$ for the ^{87}Rb is 165MHz lower than that of the ^{85}Rb. While (as described above this section) we have also redone the analysis being more careful in accounting for the FP resonance locations (in Fig.4) the previous paragraph's "sketch" of the shift measurement displays its overall simplicity.

The normal mass shift (NMS) alone for this transition (780.25nm photon's f= 3.84 x 10^{14} Hz) is found by μ-scaling, using $df/f = |d\lambda/\lambda|$ leading to $df = 57.13$ MHz. That means that the 84-57 = 27 MHz is apparently the "nuclear" part (NS) of the isotope shift between ^{85}Rb and ^{87}Rb. The best fit value for this in the literature is about 20 MHz[22] (the 7 MHz difference being apparently attributable to the SMS contribution in the $5S^{1/2}$ and $5P^{3/2}$).

Now assuming that whole NS part is due to the ground S state (since those electrons spend so much more time than non-S electrons inside the nucleus) only, we can recast the measured isotope shift into a ground state energy difference between the isotopes, relative to the continuum. The NMS part of the overall electron binding energy scales with μ, so that one can expect that part of the isotope energy difference to be the same ratio of the optical excitation energy to the known ionization energy of Rb (4.177 eV). Thus using the fact that our D2 transition at 780.25 nm has an energy of 1.59 eV, we get 57.13(4.177/1.59)+27 = 177 MHz as the NMS part of the ground state energy shift between ^{85}Rb and ^{87}Rb relative to the continuum.

For comparing excitation energies we need to compare differences of these state shifts. The reduced mass scaling for the NMS for the $5S^{1/2}$ and $5D^{5/2}$ two photon transition contributes 114.40MHz to the isotope shift. We expect the NS contribution to be the same as in the $5S^{1/2}$ and $5P^{3/2}$ transitions, being dominated by the term from the $5S^{1/2}$ common to both measurements. This then leads to an NMS+NS isotope shift contribution of about 134MHz. Thus, the only way to understand the present measurement is that the SMS contribution is about 30 MHz. Note that even if one used a naive NS measurement from the 5S-5P of 27MHz, there would still have to be a substantial additional SMS contribution. [$^{15,22?}$]) One of the strengths of this laboratory is that the easy to discern difference with the NMS+NS

alolne, the measurement idicating the necessity of including the SMS contribution.

Finally, we now report some data on student outcomes running this laboratory in the Fall 2025 in our junior/senior level course required for the physics major. We had five groups of two students each do this laboratory. Four groups sucsessfully completed the lab. One group did an "eyeball"-like estimate, not performing any functional fitting of any of the data's resonances, but simply estimating the maximum of both the lines and the FP resonances. They reported a shift of 200±40 MHz. Another group fit with symmetrical gaussians both the 776nm absorption resonances and the FP resonances and reported 166±3 MHz. Yet another group fit only the 776nm resonances and then read off the locations of the FP resonance maxima (no fit) to determine the isotope shift to be 175±10 MHz.

V. MODULATION TRANSFER SPECTROSCOPY AND THE LASER+ATOM LINESHAPE MEASUREMENT

Because it is a two-beam non-linear optical process, the multi-photon process employed here lends itself to a simple, student-friendly demonstration of modulation transfer spectroscopy. Typically in modulation transfer spectroscopy one modulates just one character of the pump field, for example either amplitude or frequency but not both. For example in Ref.[14] a mechanical chopper was used on the pump beam of the SAS modulating just the laser field amplitude. Note that the 780nm transition's doppler envelope is much wider ($\sim$ 500MHz) than both the 776nm intrinsic linewidth (a few MHz for each line and a hyperfine manifold spread of $\sim$ 20 MHz) and the 776nm free running laser linewidth (not directly measured, but also typically $<$ 10 MHz on timescales of roughly 1 mS, consistent with our observations). This means that a measurement of the 776nm laser's atomic absorption lineshape in the vapor is very nearly independent of the 780nm laser's detuning.

To measure the 776nm laser's atomic absorption lineshape we chose to directly modulate the current of the 780nm laser, in confidence that only its intensity modulation (assumed to be much slower than the $5P^{1/2}$ excited state lifetime) would imprint on the atomic response to the 776nm laser. For our measurement we lightly modulated the 780nm diode at a depth of $<$ 0.1mA at about 60 KHz with the reference provided by the lockin amplifier (SR 830) and demodulated the 776nm laser's transmission as we slew the latter's frequency at just a few Hz across the transition via a current ramp (setup as in Ref.[44]). The measured response

is the modulation transfer from one beam's frequency onto the other beam's intensity.

This approach had some notable advantages compared to the example of modulation transfer via SAS in Ref.[14]. Among them is the simplicity of not needing a reference input to the lock-in amplifier from an additional amplified photodetector (to sync for example with a mechanical chopper) and also working at a much greater modulation frequency. Primarily due to greater modulation frequency one can also complete the data capture at least an order of magnitude more quickly than using a chopper. Note that we are doing this without detecting the 420nm flourescence and not using a PMT but just the relatively common low bandwidth amplified photodiode detectors.

The output as shown in Fig. 5 is similar to the earlier absorption traces and the direct flourescence measurement data. It reveals that although the free running 776nm laser is spectrally too wide to resolve individual excited state hyperfine levels it does succeed in capturing the asymmetric (though smeared) density of states expected in the $5D^{5/2}$ hyperfine manifold.

Gaussian fits to this underlying asymmetric multi-component line are used in the analysis described earlier in this paper and so we must address how that simplification leads to systematic errors in this isotope shift measurement. First off, the finite laser linewidth tends to roughly perform a state-weighted average the underlying $5D^{5/2}$ excited state hyperfine frequencies. Second, the systematics of the structure of those states is such that interrogated from the ^{87}Rb F=2 or the ^{85}Rb F=3 the lineshape averages with almost no difference (at the *pm* 1 MHz level) between the center of the state-weighted sum and the Gaussian center.

On the other hand, the gaussian fits to the ^{87}Rb F=1 or the ^{85}Rb F=2 tends to yield a center location that apparently underestimates the actual state-averaged $5D^{5/2}$ excited state center. Including the line asymmetry of the 776nm transition connecting with the ^{87}Rb F=1 dominates this systematic source of error. Assuming that it cannot be larger than the frequency difference between the Gaussian fit center and the actual peak, our data indicates that the "center of mass" of the 87Rb line as we estimated could be as much as 3.0 MHz too low (Fig. 6). Likewise we find a fit of the 776nm transmission dip of the ^{85}Rb F=2 line data indicates an asymmetry that could result in a systematic deviation as large as 0.85 MHz. In both cases the targeted $5D^{5/2}$ excited states have the same sign of the asymmetry due to the similar "inverted" ordering of the excited hyperfine states. We then expect these systematic effects to have the same sign, and so partially cancel in the isotope

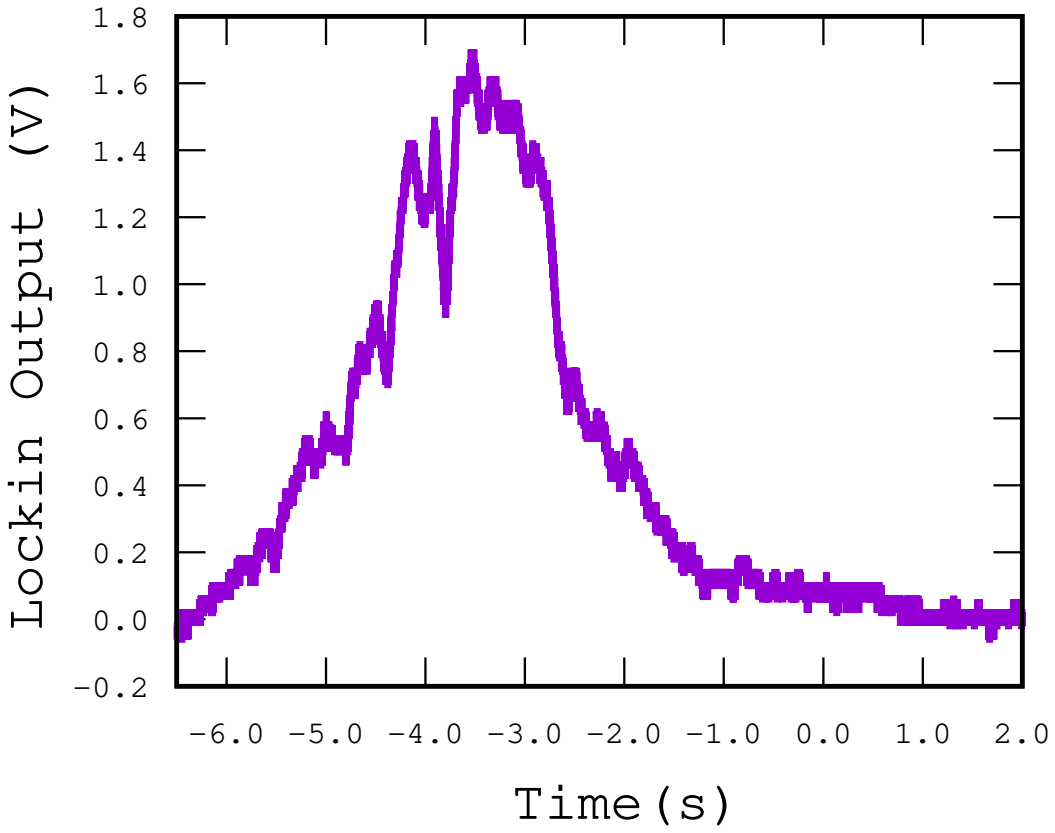

FIG. 5. Lineshape of 776nm laser on the $5D^{5/2}$ states from modulation transfer spectroscopy as described in the text. Shown is from the $5P^{3/2}$ F'=3 intermediate state of ^{87}Rb, slowly sweeping the 776nm to increasing current (so laser frequency decreases at about 10MHz/s). The asymmetry indicates the reverse ordering of the hyperfine levels (F" labels) in the $5D^{5/2}$ as compared with the $5P^{3/2}$ level, all convolved with the laser linewidths.

shift difference, leading to a systematic error about as large as the random error.

VI. CONCLUSION

It had already been established that frequency-noisy free-running laser diodes are ideal for a straightforward, pedagogically useful and inexpensive undergraduate advanced laboratory measurements. In this note we highlighted their utility in a measurement of the isotope shift in the two-photon $5S^{1/2}$-$5D^{5/2}$ transition. In particular, the narrow energy spread in the $5D^{5/2}$ hyperfine manifold allows for a simplified experimental protocol and data analysis that rather deftly achieves results with $<2\%$ random and systematic errors consistent with

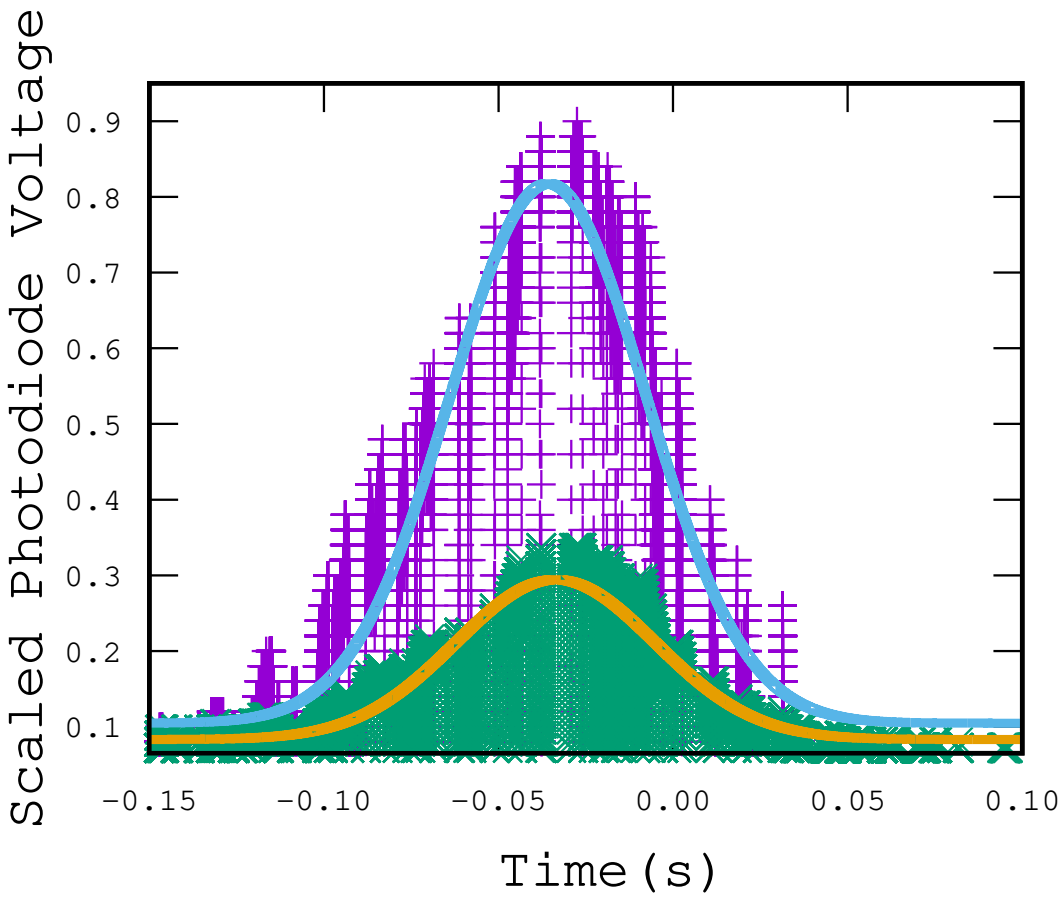

FIG. 6. Raw 776nm absorption data (purple, "+") and raw 420nm flourescence data (green, "x") of the ^{87}Rb F=1 5S-5D transition. The gaps are the result of combined laser frequency noise. The lines as the associated symmetrical gaussian fits.

the accepted value.

In addition to refining student's microphysical 'picture' of the atom, most notably, by challenging common misconceptions about the motion of the electron in the ground state, this isotope shift measurement indicates to students the necessity of including the somewhat more subtle SMS contribution. Finally, with very little modification the laboratory can demonstrate a basic use of modulation transfer spectroscopy. This laboratory's rich utility, relative setup ease and low cost will aid its future diffusion across the undergraduate experimental physics course.

ACKNOWLEDGMENTS

It is a pleasure to acknowledge discussions with I. Novikova and F. Narducci regarding this work. This work was supported in part by the U.S. National Science Foundation (Grant NSF-DMR-2226956), and the Williamson Watanakunakorn Summer Science Program at YSU.

---

* aanderson05@student.ysu.edu

† teayers@student.ysu.edu

‡ bebish@student.ysu.edu

§ sccart@student.ysu.edu

¶ vtobarcorrea@student.ysu.edu

** aobpt.sail@gmail.com

†† restipanovich@student.ysu.edu

‡‡ dcphtn@gmail.com

[1] A. C. Melisinos and J. Napolitano, "Experiments in Modern Physics," 2nd Ed., Academic Press, ISBN-10 0124898513, pgs. 233-236 (2003).

[2] A.J.Olsen, E.J. Carlson and S.K. Meyer, "Two photon spectroscopy of rubidium using a grating-feedback diode laser," Am. J. Phys, **74**(3), 218–223 (2006).

[3] D. W. Preston, "Doppler-free saturated absorption: Laser spectroscopy," Am. J. of Phys. **64**, 1432 (1996).

[4] G. P. Barwood, P. Gill, and W. R. C. Rowley, "Frequency Measurements on Optically Narrowed Rb-Stabilised Laser Diodes at 780 nm and 795 nm," Appl. Phys. B, **53**(3) 142-147 (1991).

[5] G.P. Barwood and P. Gill and W.R.C. Rowley,"An Optically Narrowed Diode Laser for Rb Saturation Spectroscopy," Journal of Modern Optics, **37**(4), 749-758 (1990).

[6] J.C. Comparo, "The laser diode in atomic physics," Contemp. Phys. **26**(5), 443–447 (1985).

[7] Ming-Sheng Ko and Yi-Wei Liu, "Observation of rubidium 5 $S_{\frac{1}{2}}$ - 7 $S_{\frac{1}{2}}$ two-photon transitions with a diode laser," Opt. Lett. **29**(15). 1799 (2004).

[8] P. Grundevik, M. Gustavsson, A. Rosen and S. Svanberg, "High Resolution Laser Fluorescence Spectroscopy in the Deep Blue Spectral Region," Z. Physik A **283**,127–132 (1977).

[9] U. Gustafsson, J. Alnis and S. Svanberg, "Atomic spectroscopy with violet laser diodes," Am. J. Phys. **68**(7), 660-664 (2000).

[10] H. S. Moon , W.-K. Lee and H. S. Suh, "Hyperfine-structure-constant determination and absolute-frequency measurement of the Rb $4D_{\frac{3}{2}}$ state," , Phys. Rev. A **79**, 062503 (2009).

[11] N. Prijapati, A.M. Akulshin, I. Novikova, "Comparison of collimated blue light generation in 85Rb atoms," arXiv:1802.07305v1.

[12] P. G. Pappas, M. M. Burns, D. D. Hinshelwood, M. S. Feld and D. E. Murnick, "Saturation spectroscopy with laser optical pumping in atomic barium," Phys. Rev. A, **21**(6) , 1955–1968 (1980).

[13] J. R. Brandenberger, "Hyperfine splittings in $4p^5$5p configuration of ^{83}Kr using saturated absorption laser spectroscopy," Phys. Rev. A **39**, 64 (1989).

[14] T.J. Bucci, J.P. Feigert, B. Chamberlain and A. Giovannone and M. Crescimanno, "Rubidium Isotope Shift Measurement using Noisy Lasers," Am. Jour. of Phys. **89**, 730 (2021).

[15] H. M. Gibbs and G. C. Churchill, "Laser spectroscopic measurement of the ^{87}Rb-^{85}Rb D_1 line isotope shift," , J. Opt. Soc. Am. **62**(10), 1130 (1972).

[16] D. E. Roberts and E. N. Fortson, "Rubidium isotope shifts and hyperfine structure by two-photon spectroscopy with a multi-mode laser," Opt. Comm., **14**(3), 332 (1975).

[17] E. Arimondo,M. Inguscio,and P. Violino, "Experimental determination of the hyperfine structure in the alkali atoms," Rev. of Modern Physics, **49**(1), 31 (1977).

[18] A. Corney, *Atomic and Laser Spectroscopy*, Clarendon Press (Oxford) 1977, Pg. 668.

[19] A. Corney, *Atomic and Laser Spectroscopy*, Clarendon Press (Oxford) 1977, Pg. 718.

[20] D. S. Hughes and C. Eckart, "The effect of the motion of the nucleus on the spectra of Li I and Li II," Phys. Rev. **3**6, 694 (1930).

[21] R. Bruch, K. Heilig, D. Kaletta, A. Stuedel, and D. Wendlandt, "Nuclear volume and mass effect in the optical isotope shift of light elements," Journal de Physique Colloques, **30** (C1), 51-C1-58 (1969).

[22] L. Aldridge, P. L. Gould, and E. E. Eyler, "Experimental isotope shifts of the 5 $^2S_{1/2}$ state and low-lying excited states of Rb," Phys. Rev. A **84** 034501 (2011).

[23] K. Mikami, M. Tanaka, Y. Yamamoto, "Probing new intra-atomic force with isotope shifts," Eur. Phys. J. C **77** 896 (2017).

[24] Y. Yamamoto, "Probing New Intra-Atomic Force with Isotope Shifts: A Neat Thing to Do,"

arXiv:1810.07146v1 (2018).

[25] Julian C. Berengut, Dmitry Budker, C´edric Delaunay, Victor V. Flambaum, Claudia Frugiuele, Elina Fuchs, Christophe Grojean, Roni Harnik, Roee Ozeri, Gilad Perez, and Yotam Soreq "Probing New Long-Range Interactions by Isotope Shift Spectroscopy," Phys. Rev. Lett., **120**, 091801,(2018).

[26] Y. Kato and B. P. Stoicheff, "Two-photon absorption to highly excited D states of Rb atoms, " J. Opt. Soc. Am., **66**(5), 490–492 (1976).

[27] F. Nez, F. Biraben, R. Felder and Y. Millerioux, "Optical frequency determination of the hyperfine components of the $5S_{1/2}$-$5D_{3/2}$ two-photon transitions in rubidium," Opt. Comm. **102** 432-438 (1993).

[28] C. Glaser, F. Karlewski, J. Kluge, J. Grimmel, M. Kaiser, A. Günther, H. Hattermann, M. Krutzik and J. Fortágh, "Absolute frequencey measurement of rubidium 5S-6P transitions," Phys. Rev. A. **102**, 012804 (2020).

[29] J. Blue, S. B. Bayram, and S. D. Marcum, "Creating, implementing, and sustaining an advanced optical spectroscopy laboratory course," Am. J. Phys. **78**, 503 (2010).

[30] C. Leahy, J. T. Hastings, P.M. Wilt, "Temperature dependence of Doppler broadening in rubidium:an undergraduate experiment," Am J. Phys, **65**(5) 367 (1987).

[31] A. J. Hachtel, J. D. Kleykamp, D. G. Kane, M. D. Marshall, B. W. Worth, J. T. Barkeloo, J. C. B. Kangara, J. C. Camenisch, M. C. Gillette, and S. Bali "An undergraduate measurement of radiative broadening in atomic vapor," Am. J. Phys. **80**, 740 (2012).

[32] V. Jacques, B. Hingant, A. Allafort, M. Pigeard and J. F. Roc, "Nonlinear spectroscopy of rubidium:an undergraduate experiment," Eur. J. Phys. **30** 921—934 (2009).

[33] C. H. H. Schulte, G. M. Müller, H. Horn, J. Hübner, and M. Oestreicha, "Analyzing atomic noise with a consumer sound card," Am. J. Phys. **80**, 240 (2012).

[34] B. E.Sherlock and I. G. Hughes, "How weak is a weak probe in spectroscopy?" Am. J. Phys. **77**(2) 111–115 (2009).

[35] D. A. Smith and I. G. Hughes, "The role of hyperfine pumping in multilevel systems exhibiting saturated absorption," Am. J. Phys. **72**(5), 631–637 (2004).

[36] B. Ohayon, H. Rahangdale, A. J. Geddes, J. C. Berengut and G. Ron, "Isotope shifts in ^{20,22}Ne: Precision measurements and global analysis in the framework of intermediate coupling," Phys. Rev. A, **99**, 042503 (2019).

[37] A. O. Neely, K. Cassella, S. Eustice, D. M. Stamper-Kurn, "Isotope shifts in the metastable a^5F and excited y^5G^0 terms of atomic titanium," Phys. Rev. A, **103**, 032818 (2021).

[38] R. D. Cowan, "The Theory of Atomic Structure," 1st Ed. , ISBN 9780520038219, pgs 505-506 (1981).

[39] Y. Accad, C. L. Perkeris, and B. Schiff, "S and P states of the Helium isoelectronic sequence up to Z-10," Phys, Rev. A **4**, 516 (1971).

[40] L. A. Bloomfield, H. Gerhardt, and T. Hänsch, "Specific mass shift in the $1s2s^3S$ and $1s5p^3P$ states of helium," Phys. Rev. A., **27**(4), 2261 (1983).

[41] X. Qi, P. Zhang, Z. Yan, G. W. F. Drake, A. Chen, Z. Zhong, and T. Shi, "Theoretical calculations for isotope shifts of $^{7,9,10,11,12,14}Be^{2+}$ ions," Phys. Rev. A textbf 110, 012810 (2024).

[42] https://www.youtube.com/shorts/JIpMK_TIzHo

[43] https://github.com/docphoton/arduinoLaserTemperatureController

[44] M. Schmitt , E. A. L. Henn , J. Billy , H. Kadau , T. Maier , A. Griesmaier and T. Pfau, "Spectroscopy of a narrow-line optical pumping transition in dysprosium," Opt. Lett., **38**(5), 637–639 (2013)